WATER PRODUCTION MODELS FOR COMET BRADFIELD (1979ℓ)*

H. A. Weaver and P. D. Feldman
Physics Department
Johns Hopkins University
Baltimore, Md. 21218

M. C. Festou
Space Physics Research Laboratory
University of Michigan
Ann Arbor, MI. 48109

ABSTRACT

IUE observations of Comet Bradfield (1979ℓ) made from 10 January 1980 to 3 March 1980 permit a detailed study of water production for this comet. Brightness measurements are presented for all three water dissociation products, H, O, and OH, and comparisons are made with model predictions. The heliocentric variation of the water production rate is derived.

INTRODUCTION

Recent observations of Comet Bradfield (1979ℓ) have convincingly demonstrated the advantages of the IUE for the study of comets. In particular, these IUE observations allow an in-depth study of the production of water, the presumed primary constituent of the cometary nucleus, as all three water dissociation products, H, O, and OH, were observed simultaneously. The excellent pointing capability of the instrument and the ability to obtain spatial imaging within the 10" x 20" aperture allowed us to map the brightness across the coma for each species at a resolution of ~1000 km, thus facilitating comparisons with model predictions. Comet Bradfield was observed at least once a week from 10 January 1980 to 3 March 1980 enabling us to follow the variation in the water production rate as the comet's heliocentric distance increased from 0.71 a.u. to 1.53 a.u. This provided another important insight into the nature of cometary phenomena.

MODEL

A radial outflow model (ref. 1) was used to interpret the data and to calculate water production rates. This is a spherically symmetric model which assumes that all species flow radially outward from the nucleus with a constant speed. The outflow velocities and characteristic lifetimes against destruction for the given atoms or molecules are the input parameters and the model then gives the density of the species as a function of distance from

*Work supported by NASA grant NSG-5393.

the nucleus. Densities are converted to column densities which are then related to surface brightness, assuming resonant scattering or resonance fluorescence to be the only important excitation mechanism for ultraviolet emission.

Figure 1 shows a comparison of model and observation for OH. The labels A and B refer to the same model but using different input parameters for v_{H_2O} and τ_{OH}. A more exact model (ref. 2), taking into account the spatial distribution of the dissociation fragments, gives essentially the same fit to the data. The derived OH production rate, Q_{OH}, depends on the chosen input parameters. It was obtained from the absolute OH brightness measurement using an excitation factor for resonance fluorescence (g-factor) calculated by A'Hearn et al. (ref. 3). Unfortunately, brightness data at projected distances $>10^5$ km are needed to choose between the two curves shown.

DISCUSSION

The study of the OH (and presemably H_2O) production rate vs. heliocentric distance shown in Fig. 2 produced some interesting and rather surprising results. It is usually assumed that this variation has an r^{-2} dependence, based on the concept that the comet's absorption of solar radiation controls the vaporization of gas from the nucleus. Our result that the production rate decreases as $r^{-3.7}$ is in disagreement with this assumption and is also quite different from the results derived from OAO-2 observations of Comets Bennett (1970 II) and Tago-Sato-Kosaka (1969 IX) (refs. 4, 5).

While the OH emission is optically thin, this is not the case for the Lyα emission of atomic hydrogen. An approximate radiative transfer calculation is used (ref. 6) to relate the measured surface brightness to column density for comparison with the model. Since our measurements are confined to regions relatively close to the nucleus we neglect radiation pressure. The data, shown in Fig. 3, are in reasonably good agreement with predictions based on the derived Q_{OH} values.

In principle we can use oxygen to distinguish between models A and B because O will be twice as abundant when τ_{OH} is half as large. However, the oxygen problem is complicated by other factors. First, it is difficult to calculate an accurate g-factor as the cometary absorption wavelength is doppler-shifted into a steeply-sloped portion of the corresponding solar line (ref. 7). Also, since the absorption takes place from a ^3P term, it is necessary to know the relative populations of the fine structure levels of the ground state. Finally, it appears that the oxygen emission is barely optically thick.

Nevertheless, some qualitative information about the source of the oxygen may be obtained from an examination of the spatial variation of the oxygen, both from offset exposures and from variation within the aperture itself. Oxygen produced from a second dissociation:

$$H_2O + h\nu \rightarrow OH + H$$

$$OH + h\nu \rightarrow O + H$$

leads to an integrated column density which is independent of projected distance near the nucleus. The data, however, show a variation in brightness near the nucleus indicating a direct dissociation source of oxygen. Two possibilities immediately come to mind. Oxygen in the ground state may be produced from direct photodissociation of H_2O via the reactions:

$$H_2O + h\nu \rightarrow O[(^1D) \text{ or } (^1S)] + H_2$$

$$O[(^1D) \text{ or } (^1S)] \rightarrow O(^3P) + h\nu.$$

The presence in our spectra of the "trans-auroral" oxygen line at 2972 Å suggests that such a process may play a role in oxygen production. If this photodissociation channel operates at a 10% efficiency level (ref. 2) (with 90% of the H_2O dissociating into OH + H) then the agreement between model predictions and the data is much better than for the case when only a second dissociation is considered (see Fig. 4). The other possibility is a source of O which is <u>not</u> water. Likely candidates are CO and CO_2. An estimate of their importance may be obtained by reference to the carbon emission lines also present in the spectrum.

CONCLUSION

The data presented here represent a small sub-set of all the Comet Bradfield observations containing spatial information about the water dissociation products. Continuation of this analysis with the remaining data should serve to place further constraints on water production models for comets.

REFERENCES

1. Haser, L.: Distribution d'intensité dans la tête d'une comète. Bull. Acad. Roy. Belgique, 43, 740-750, 1957.

2. Festou, M.: The Density Distribution of Neutral Compounds in Cometary Atmospheres II. Production Rate and Lifetime of OH Radicals in Comet Kobayashi-Berger-Milon (1975 IX). Submitted to Astron. and Astrophys., 1980.

3. A'Hearn, M. F.; Schleicher, D. G.; Donn, B.; and Jackson, W.: Fluorescence Equilibrium in the Ultraviolet Spectra of Comets Seargent (1978m) and Bradfield (1979ℓ). The Universe in Ultraviolet Wavelengths: The First Two Years of IUE. NASA CP- , 1980. (Paper of this compilation).

4. Keller, H. U.; and Lillie, C. F.: The Scale Length of OH and the Production Rates of H and OH in Comet Bennett (1970 II): Astron. and Astrophys., 34, 187-196, 1974.

5. Keller, H. U.; and Lillie, C. F.: Hydrogen and Hydroxyl Production Rates of Comet Tago-Sato-Kosaka (1969 IX). Astron. and Astrophys., 62, 143-147, 1978.

6. Festou, M.; et al.: Lyman-alpha Observations of Comet Kobayashi-Berger-Milon (1975 IX) with Copernicus, Astrophys. J., 232, 318-328, 1979.

7. Feldman, P. D.; Opal, C. B.; Meier, R. R.; and Nicolas, K. R.: Far Ultraviolet Excitation Processes in Comets. The Study of Comets, ed. B. Donn et al. NASA SP-393, 773-795, 1976.

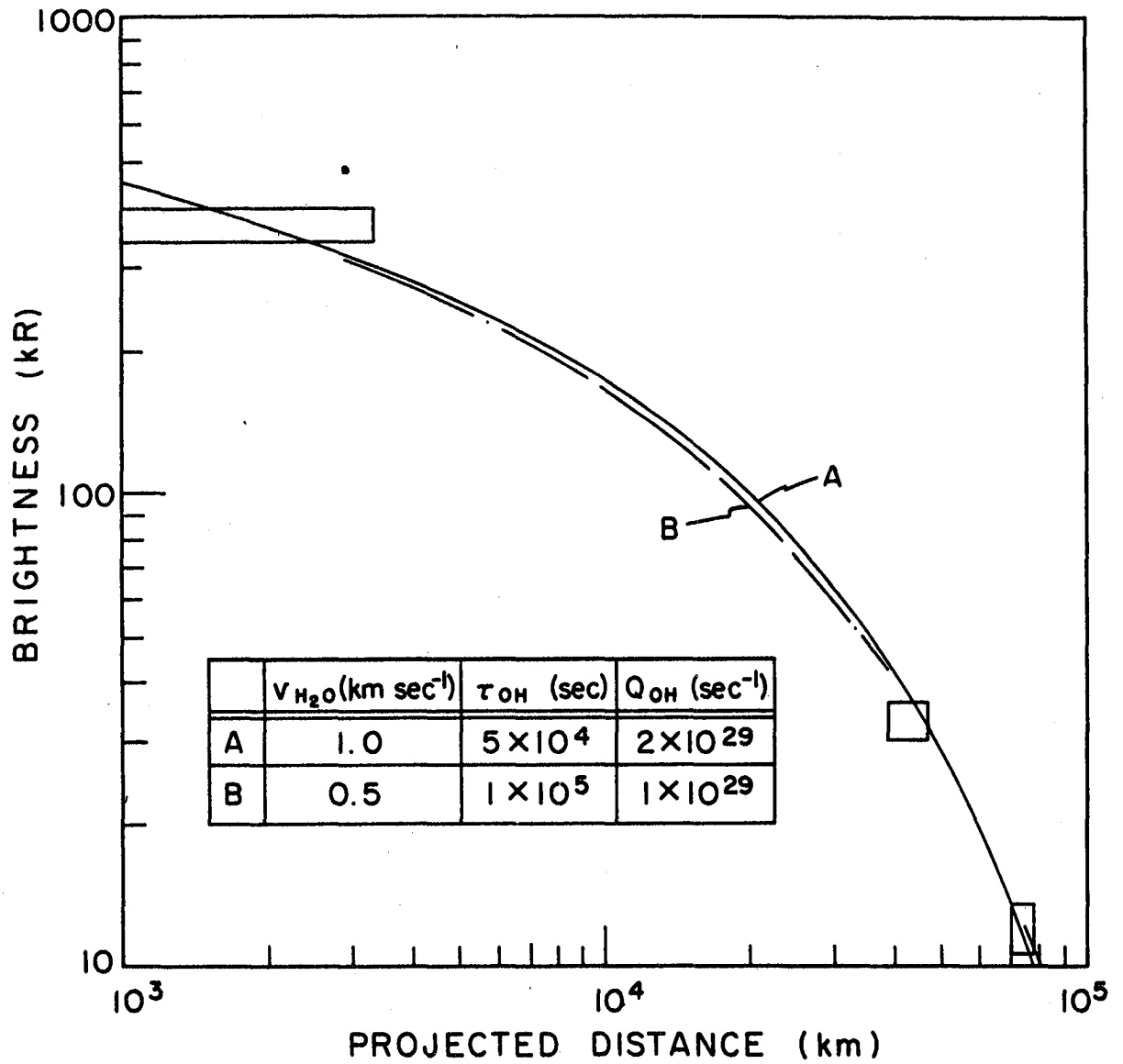

Fig. 1. Comparison of the OH (0,0) band brightness profile with a radial outflow model using the parameters defined in the insert. Data from three exposures are shown as rectangular boxes, the horizontal size being the projected length of the spectrograph slit on the comet and the vertical size the measurement uncertainty.

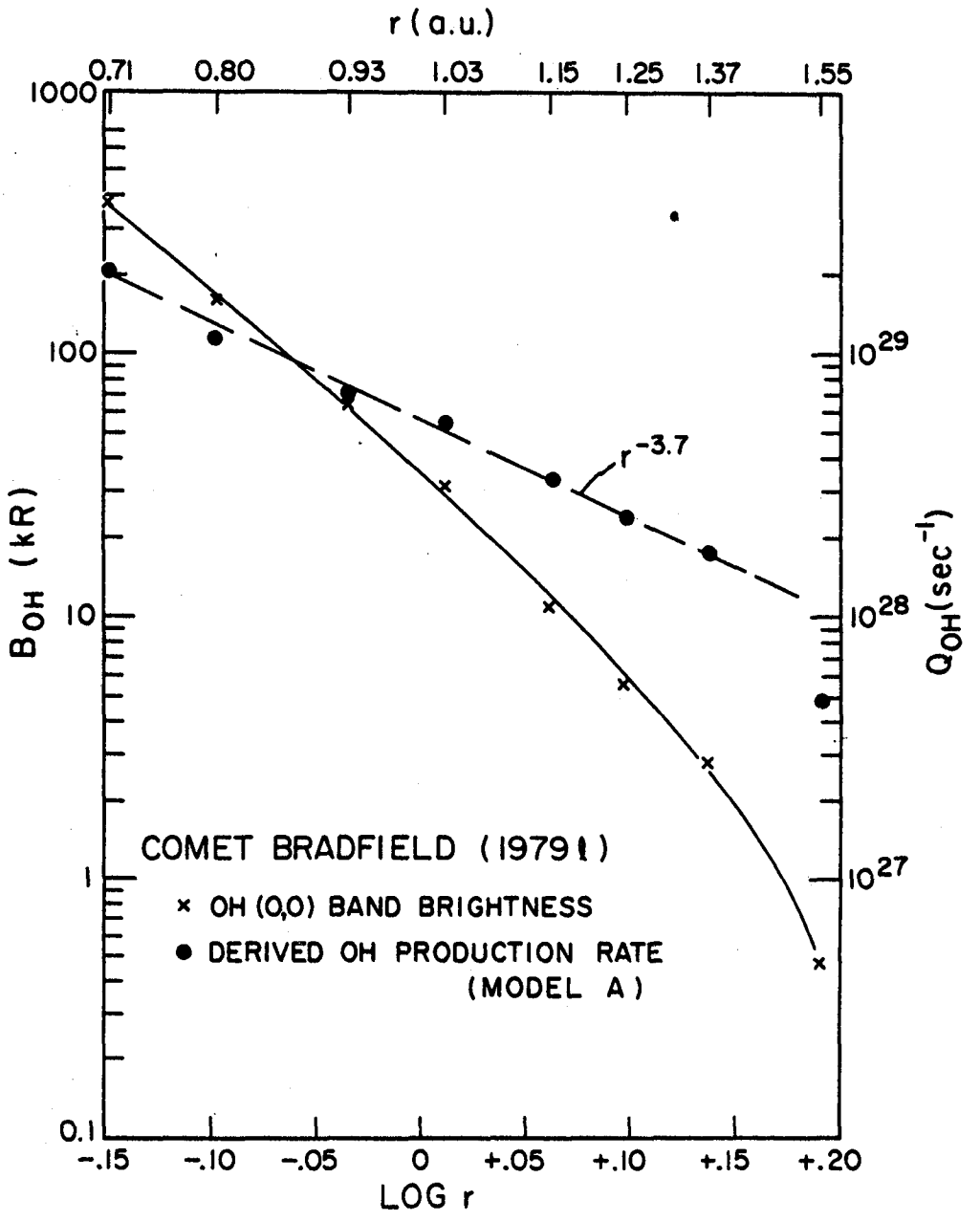

Fig. 2. Brightness of the OH (0,0) band as a function of heliocentric distance. Also shown is the derived OH production rate using model A. Model B reduces the production rate by a factor of two for each measurement but leaves the slope unchanged.

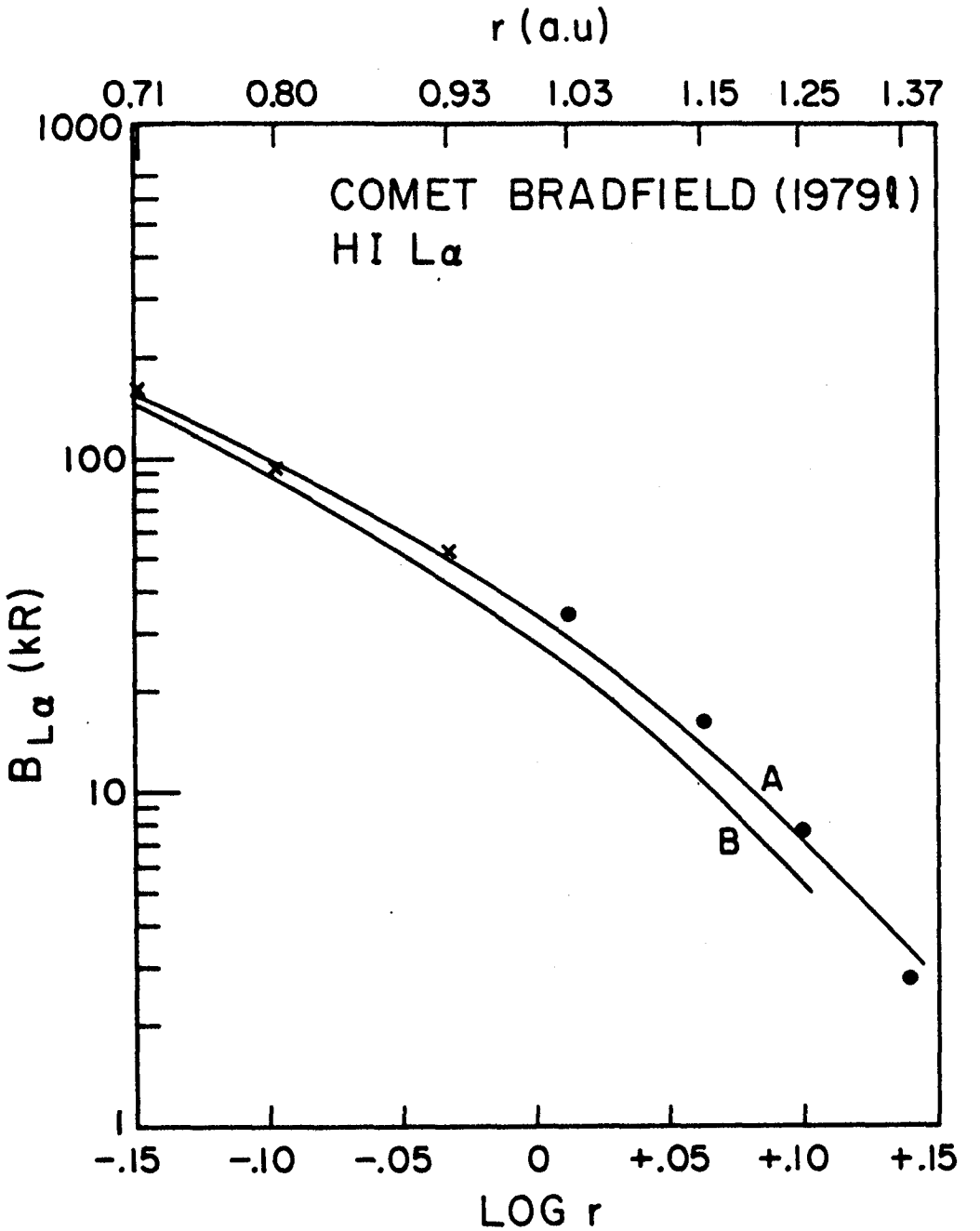

Fig. 3. The two curves show the predicted HI Lα brightness as a function of heliocentric distance using models A and B and H_2O production rates derived from the OH measurements. The plotted points represent the measured values. The dots include a subtraction of geocoronal Lα while the x's do not.

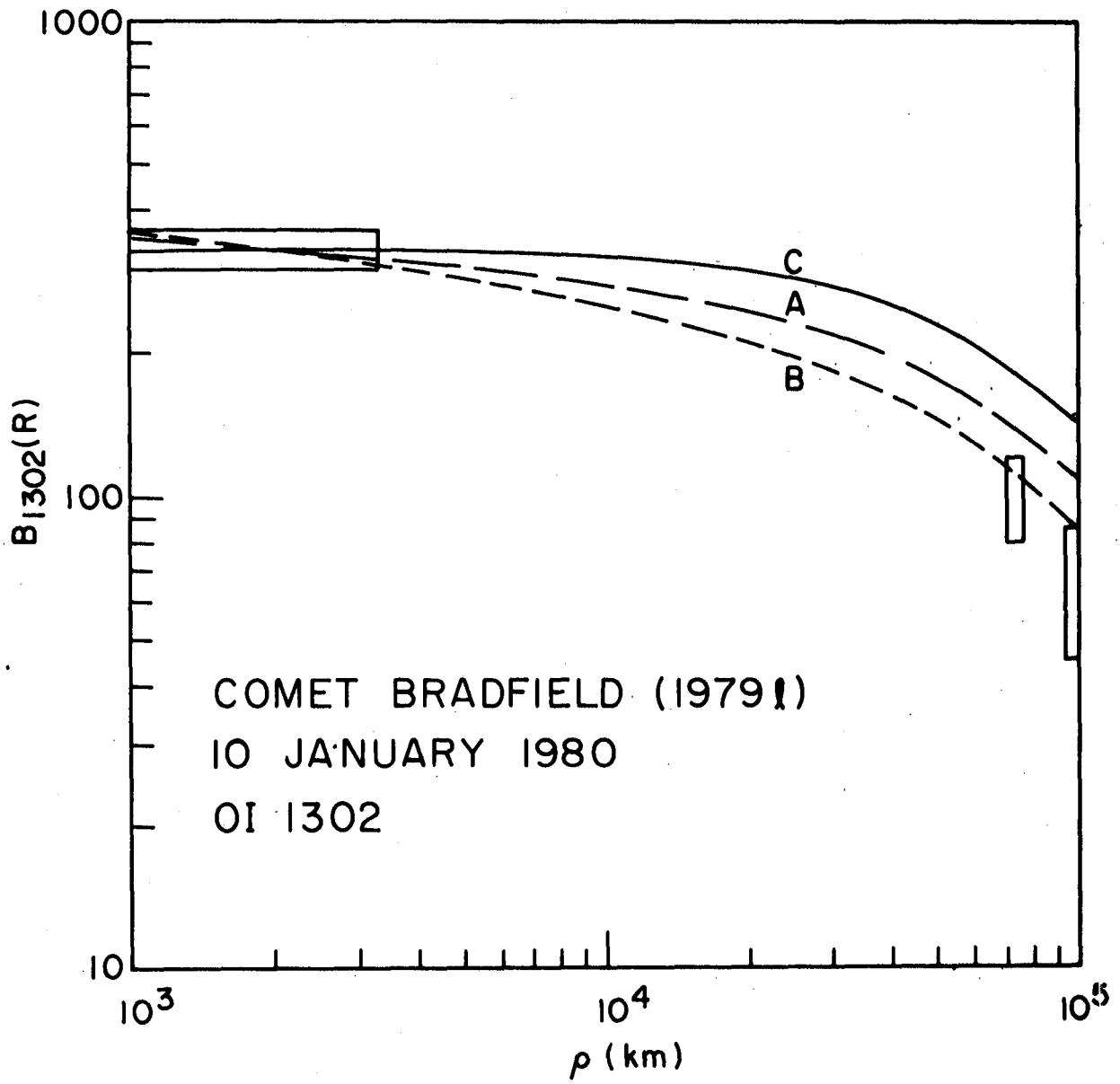

Fig. 4. Comparison of the O(1302 Å) brightness profile with model predictions. All three curves have been normalized to the observed average brightness obtained with the aperture centered on the nucleus. Curves A and B are the same as in Fig. 1 and assume a 10% branching ratio for direct production of O. Curve C is for zero branching and is the same for both models.